High Power Factor Control of Brushless DC Motor Drive System without Electrolytic Capacitor

Xiaoyu Jiang [1], Jianbo Chu [1] and Fan Li [1]
[1]Electrical engineering, College of Automation Engineering, Nanjing University of Aeronautics & Astronautics, China
E-mail: nuaachu@nuaa.edu.cn

***Abstract*--This paper proposes a novel control strategy for the brushless DC motor drive system fed by electrolytic capacitor-less inverter. In order to obtain high power factor, this paper proposes a new control method that regulates the inverter input current. The calculated compensation current of small film capacitor is subtracted from the ideal ac input current, which is regarded as the ideal inverter input current. The inverter input current is regulated by a PI controller, and the output of PI controller is used as duty-cycle of PWM technique. Meanwhile, the PWM_ON_PWM pattern is used in the proposed system, which can reduce the torque ripple in BLDCM. The effectiveness of the proposed system has been verified by simulation and experiment.**

***Index Terms*—BLDCM, non-electrolytic capacitor, power factor, square-wave drive system.**

I. INTRODUCTION

In general, large-capacity electrolytic capacitors are placed between single-phase diode rectifiers and three-phase voltage source inverters in the single-phase to three-phase power converters, which can maintain a constant DC-link voltage. However, the electrolytic capacitors in the inverter circuit occupy a large volume, and its lifetime is greatly affected by the increase of temperature. To solve these problems, small film capacitors are used to replace the electrolytic capacitors in the single-phase to three-phase power converters, and many new control methods are proposed to improve the power factor [1]-[2]. Comparing with conventional motor drive system, the new motor drive system without electrolytic capacitor has the advantages of long service life, small volume, low cost, and so forth. At present, the IPMSM system which driven by E-caps-less inverter has been extensively studied to apply in household air conditioner compressor system [3]-[5].

Compared with PMSM, BLDCM has the advantages of sample control structure, high voltage utilization and broad adjustable-speed range, and so on. Moreover, it has been widely used in home appliance, automobile, aviation and other industries in recent years. The traditional control technology of BLDCM has been mature, which focuses on the following aspects: first, doing the research about position sensor-less control methods to improve the reliability of the system, and reduce the volume and weight of the motor further [6]-[7]; second, studying torque ripple suppression techniques to improve the servo precision [8]-[9]; third, looking out for a novel and sample flux weakening control of BLDCM [10]-[11].

Nevertheless, the research on the BLDCM drive system without electrolytic capacitor is very little [12]. Accordingly, this paper applies the E-caps-less inverter to BLDCM drive system, to solve the problem of short life caused by the large electrolytic capacitor effectively. Meanwhile, by putting forward a novel strategy, the high input power factor can be achieved.

II. TRADITIONAL E-CAPS-LESS CONTROL STRATEGY

The classic topology structure of PMSM drive system without electrolytic capacitor is shown in Fig.1. The DC-link capacitor is changed from electrolytic capacitor with large capacity to thin-film capacitor, which reduces the system size and improves the service life at the same time.

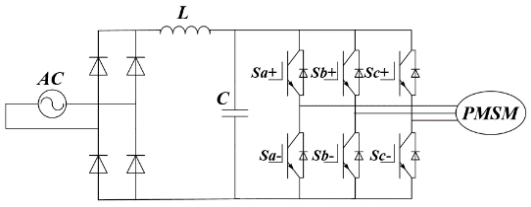

Fig.1. New power converter without electrolytic capacitor.

Nevertheless, the small capacitance may lead to the DC-link voltage fluctuation, which causes the increase of input current harmonic and the decrease of input power factor, with the control difficulty increases greatly. In order to improve the power factor, two control strategies have been proposed: the control scheme based on inverter input current tracking and inverter output power tracking.

For two control strategies, the given current of d-axis are both the negative value, which used to achieve the flux-weakening control. The biggest difference is the given current of q-axis. A brief introduction of these two approaches is as follow.

A. Inverter input current control

When the input current is sinusoidal and its phase is the same as the input voltage, the input factor is close to 1. Therefore, it is natural to take current tracking into consideration.

978-1-5386-3246-8/17/$31.00 2017 IEEE

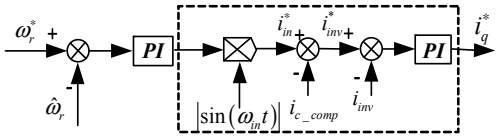

Fig.2. Control block diagram.

The control method is shown in Fig.2. The error of the DC-link current command i^*_{inv} and its feedback signal i_{inv} is inputted to the PI controller, and the output is the q-axis current command i^*_q . However, it is difficult to achieve a good tracking performance by using a PI controller only due to a change near the zero-crossing. The tracking performance can be improved through the use of repetitive control technique in theory.

B. Inverter output power control

Due to the problem of the inverter input current feedback control method mentioned above, the inverter output power feedback control method is proposed. Fig.3 shows a block diagram for controlling the inverter output power.

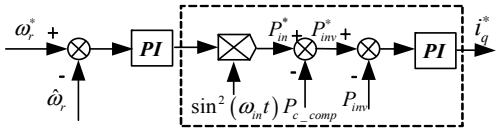

Fig.3. Control block diagram.

The input power command P^*_{in} is determined by multiplying the output of the speed controller with $\sin^2(\omega_{in}t)$ generated from the ac input voltage. The inverter output power command P^*_{inv} is calculated by subtracting the compensation power of the DC-link capacitor P_{c_comp} from the input power command P^*_{in}. The inverter output power P_{inv} is equals to the apparent power of machine, when the power consumed by the rectifier and inverter is neglected. When the error in P_{inv} is inputted to the PI controller, the output is the q-axis current command i^*_q .

In this control method, the change in the inverter output power at the zero-crossing of the input voltage is smooth and insignificant, thus a good tracking performance of inverter output power can be achieved easily by using a PI controller. Furthermore, the PR controller can be used to improve the tracking performance, both of the PI controller and the PR controller are easier than the repetitive control technique.

III. An Electrolytic Capacitor-less BLDCM Drive Method

Fig.4 shows a block diagram for traditional control method of BLDCM. The inner-loop of the scheme is inverter input current feedback control and outer-loop is motor's speed feedback control. The speed and current are regulated by the PI controllers, and the output signal of current loop controller is used as *Duty*, which is used to control the inverter output voltage.

The DC-link voltage generates ripples when the DC-link capacitor is changed from electrolytic capacitor with large capacity to thin-film capacitor. And it causes the increase of input current harmonic and the decrease of input power factor, with the control difficulty increases greatly.

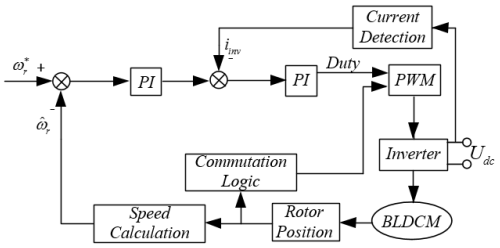

Fig 4. Control block diagram of traditional BLDCM drive system.

A. Proposed method

In order to improve the power factor, a novel control strategy is proposed in this paper. Fig.5 shows the proposed block diagram for the obtainment of duty-cycle.

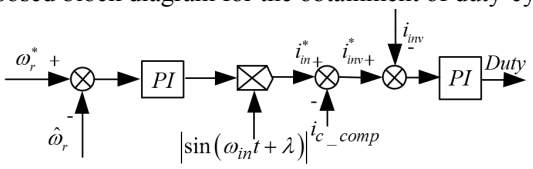

Fig 5. The obtainment of duty-cycle.

The detailed analysis is as follows:

For the purpose of a high power factor, the input current must be sinusoidal and its phase must be the same as the input voltage.

The signal of ac input voltage is a sine wave.

$$v_{in} = \sqrt{2}U\sin(\omega_{in}t) \tag{1}$$

Where, v_{in} is the single phase ac input voltage, U is the ac voltage RMS, ω_{in} is the angular velocity of ac voltage.

Suppose the input power factor is unity, thus the ideal ac input current is shown as (2).

$$i^*_{in} = \sqrt{2}I\sin(\omega_{in}t) \tag{2}$$

Where, i^*_{in} is the single phase ac input voltage, I is the ac voltage RMS, ω_{in} is the angular velocity of ac voltage.

The compensation current of the DC-link capacitor is calculated as (3).

$$\begin{aligned} i_{c\_comp} &= C\frac{d|V_{in}|}{dt} \\ &= \sqrt{2}CU\omega_{in}\cos(\omega_{in}t)\,sign(\sin(\omega_{in}t)) \end{aligned} \tag{3}$$

Where, sign is the sign function.

$$sign(x) = \begin{cases} 1 & (x>0) \\ 0 & (x=0) \\ -1 & (x<0) \end{cases} \tag{4}$$

We can make a node equation from eq. (2), (3) in Fig. 5. The node equation is following.

$$
\begin{aligned}
i_{inv}^{*} &= \left|i_{in}^{*}\right| - i_{c\_comp} \\
&= \left|\sqrt{2} I \sin\left(\omega_{in} t\right)\right| \\
&\quad - \sqrt{2} C U \omega_{in} \cos\left(\omega_{in} t\right) sign\left(\sin\left(\omega_{in} t\right)\right)
\end{aligned} \tag{5}
$$

The relationship between each current is shown in Fig. 6. There is a change near the zero-crossing in i_{inv}^{*}, so it is difficult to achieve a good tracking performance by using a PI controller only. In theory, the tracking performance can be improved through the use of repetitive control technique.

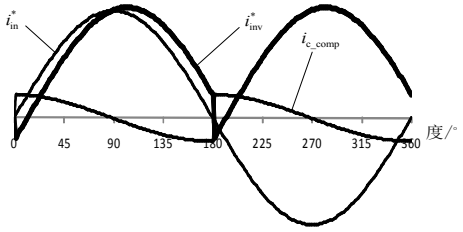

Fig.6. Current command waveforms.

Furthermore, the signal of the inverter input current is a high-frequency chopper in square-wave drive system. The i_{inv} is detected after the switching frequency band is rejected by a low-pass filter. The phase delay of i_{inv} due to the low-pass filter leads to a low power factor. For this reason, a phase compensation method is needed to phase the ac input voltage and the ac input current. The phase delay caused by the low-pass filter is shown in (6).

$$
\lambda = -\arctan\left(\frac{f}{f_c}\right) \tag{6}
$$

Where, f is the frequency of the input signal, f_c is the cut-off frequency of the filter.

Finally, i_{inv}^{*} is described according to (7).

$$
\begin{aligned}
i_{inv}^{*} &= \left|i_{in}^{*}\right| - i_{c\_comp} \\
&= B\left|\sin\left(\omega_{in} t + \lambda\right)\right| \\
&\quad - \sqrt{2} C U \omega_{in} \cos\left(\omega_{in} t\right) sign\left(\sin\left(\omega_{in} t\right)\right)
\end{aligned} \tag{7}
$$

Where, B is the output signal of speed loop controller, λ is the phase compensation.

B. PWM mode

The BLDCM typically is driven based on commutation of every 60 electrical degrees. There are four pulse-width modulation (PWM) techniques: PWM_ON pattern, ON_PWM pattern, H_PWM_L_ON pattern, H_ON_L_PWM pattern and H_PWM_L_PWM pattern. These traditional modulation methods have their advantages and disadvantages.

(1) PWM_ON: The switch losses are evenly distributed and this pattern achieves the smallest torque ripple. Nonetheless, the diode freewheeling of inactive phase can increase the torque ripple to some extent.

(2) H_PWM_L_PWM: The switch losses are double, and the torque ripple is biggest within these. While there is no diode freewheeling of inactive phase only in this pattern.

(3)The torque ripple caused by other patterns is between these two patterns above, and there all has diode freewheeling of inactive phase.

Fig.7 shows the PWM_ON_PWM pattern, which is proposed by integrating all these advantages above. Compared with PWM_ON, there is no diode freewheeling of inactive phase in this pattern. So, no additional torque ripple will be generated.

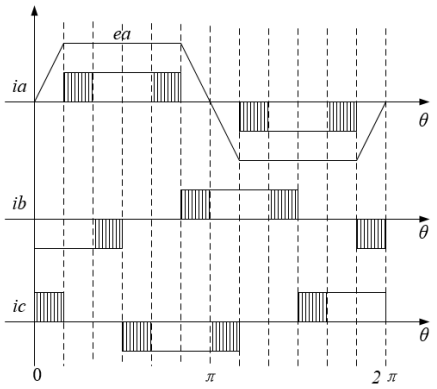

Fig 7. Switching pattern of conventional PWM_ON_PWM technique.

According to Fig.8, take the case of the cut-off time of A phase. The three-phase terminal voltages are shown in (8).

$$
\begin{aligned}
U_a &= ea + U_N \\
U_b &= U_{dc} S_b = R i_b + L \frac{di_b}{dt} + eb + U_N \\
U_c &= U_{dc} S_c = R i_c + L \frac{di_c}{dt} + ec + U_N
\end{aligned} \tag{8}
$$

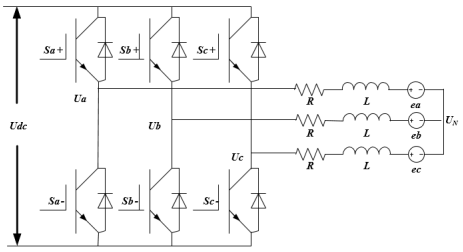

Fig 8. Equivalent circuit mode.

Where, U_b, U_c represents the terminal voltage of the corresponding winding. $S_b/S_c = 0$ means that the down bridge arm turns on or diode freewheeling; $S_b/S_c = 1$ means that the up bridge arm turns on or diode freewheeling. According to $i_b = -i_c$ and $eb = -ec$, the neutral-point voltage is shown in (9).

$$
U_N = \frac{1}{2} U_{dc}\left(S_b + S_c\right) \tag{9}
$$

The terminal voltage of non-conducting phase is described in (10).

$$U_a = ea + \frac{1}{2}U_{dc}\left(S_b + S_c\right) \tag{10}$$

In the interval of 0~π/6, there are $0 \le ea \le 0.5U_{dc}$ and $S_b = 0, S_c = 1/0$ from Fig. 8. Therefore, the terminal voltage of A phase U_a is greater than zero and less than the DC-link voltage. It means that the diode doesn't go through and there is no diode freewheeling. Similarly, there are the same conclusion in 5π/6~π, π~7π/6, and 11π/6~2π. As a result, there is no diode freewheeling of inactive phase in BLDCM drive system by using the PWM_ON_PWM pattern. From the overall performance, PWM_ON_PWM is better than the conventional patterns.

In the proposed system, the torque ripple may increase the pulsation of ac input current, even dropped to zero. This will causes the increase of input current harmonic and the decrease of input power factor. Finally, the PWM_ON_PWM pattern is chose as the PWM generator due to its minimal torque ripple.

C. Flux-weakening control

In this proposed system, the higher power factor is obtained when the ripple band of the DC-link voltage is larger. So in order to ensure the stable running of the electric machine when the DC-link voltage is small, the flux weakening control method is necessary.

The traditional flux wakening control of BLDC is leading angle flux weakening control. It makes the phase current *i* leading the back EMF *e*, as shown in Fig 9.

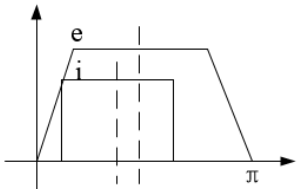

Fig 9. Relation curves between *i* and *e*.

D. Control block diagram

Fig.10 shows the system configuration and the proposed control block diagram. In the proposed system, the "*Commutation Logic*" is used to determine the switch state of the power tube, which is selected by the rotor position and the leading angle of flux weakening control. The inverter driving signal is generated by the module of "PWM". It is controlled by the output value of "*Commutation Logic*", the duty cycle Duty, and the PWM_ON_PWM pattern. The rest is covered in the previous content.

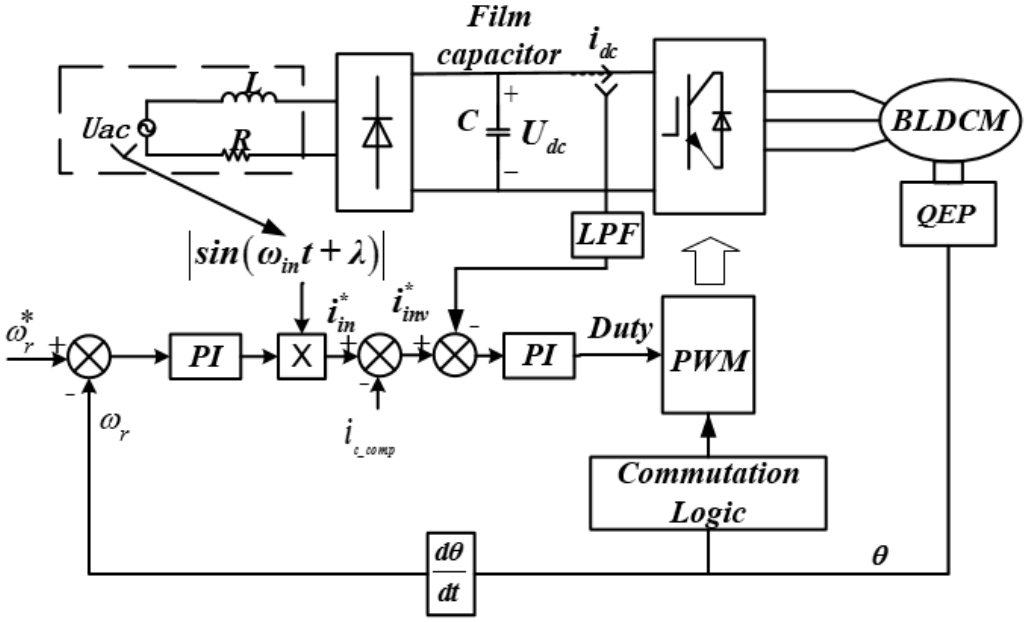

Fig 10. Control block diagram of proposed system.

IV. Simulation Results

In order to verify the effectiveness of the proposed control method, a computer simulation model is developed by using the PLECS. In the simulation, the source voltage sets at 50[Hz] and 220[V], and the DC-link thin capacitor sets at 20[μF]. The BLDCM parameters used in the simulation are listed in Tables 1.

In this simulation, motor speed is 2000, 3000 rpm and load torque is 0.5, 2 N.m. Fig.11-18 show the power factor and the tracking performance of the simulation results of the proposed methods. Fig.11 and 13 show the input voltages and the input currents of the proposed method at 2000 rpm according to load torques. And Fig.12 and 14 show the tracking performance of the inverter input current of the proposed method. Fig.15 and 17 show the input voltages and the input currents of the proposed method at 3000 rpm according to load torques. And Fig.16 and 18 show the tracking performance of the inverter input current of the proposed method.

The results of simulation list in Table 2. As shown in Table 2, the power factor characteristic is good not only

heavy load condition but also light load condition.

Table 1.

Motor parameters	
Stator resistance (R_s)	1.07[ohm]
d-axis inductance (L_d)	8.0[mH]
q-axis inductance (L_q)	10.8[mH]
Pole number	6
Inertia(J)	3.2e-4[kg.m^2]
Linkage flux (ϕ_f)	0.109[Wb]

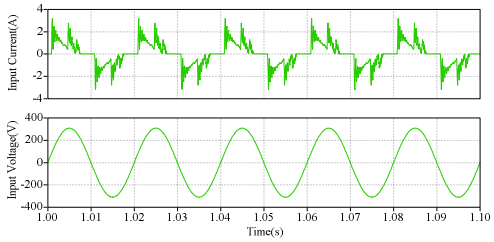

Fig.11. Input voltage and input current. (2000rpm, 0.5N.m)

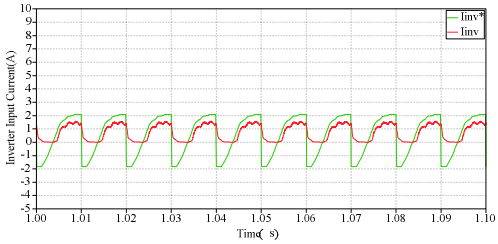

Fig.12 Inverter input current. (2000rpm, 0.5N.m)

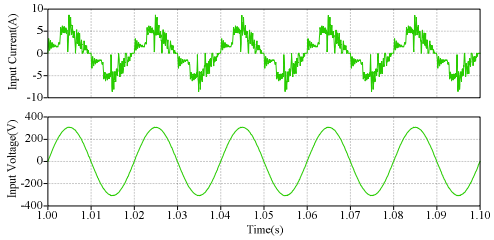

Fig.13. Input voltage and input current. (2000rpm, 2N.m)

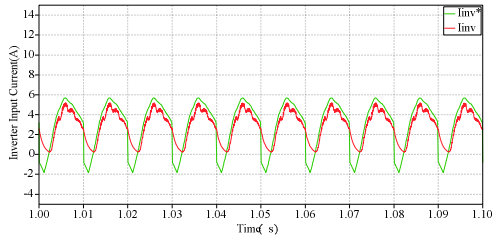

Fig.14. Inverter input current. (2000rpm, 2N.m)

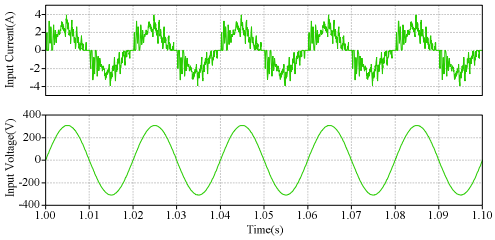

Fig.15 Input voltage and input current. (3000rpm, 0.5N.m)

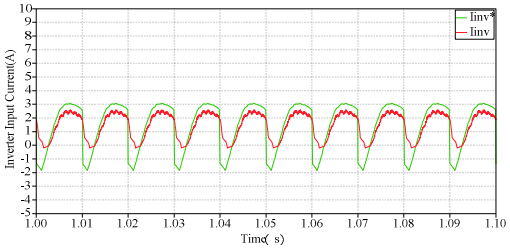

Fig.16 Inverter input current. (3000rpm, 0.5N.m)

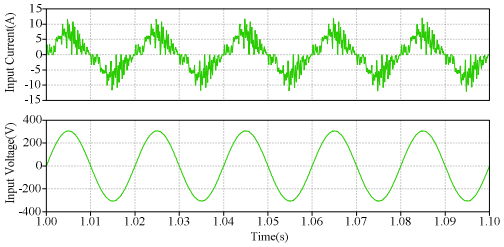

Fig.17. Input voltage and input current. (3000rpm, 2N.m)

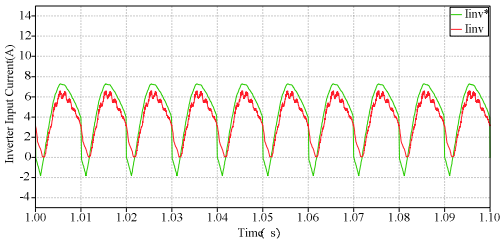

Fig.18. Inverter input current. (3000rpm, 2N.m)

Table 2.

PF	0.5N.m	2N.m
2000rpm	0.79	0.913
3000rpm	0.903	0.924

V. Experimental Results

The experiment system is established based on a TMPM470FDFG board, and the input power factor is calculated by using a PowerBay. The experiment data prove the veracity of the proposed control strategy. Fig.19-22 show the input voltages and the input currents of the experimental results of the proposed methods. And the power factor of the experimental results are listed in Table 3. The experimental results are almost accordant with the simulation results. And the proposed method with the inverter input current feedback achieves a high power factor.

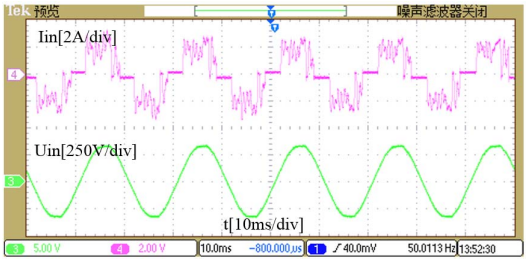

Fig.19 Input voltage and input current. (2000rpm, 0.5N.m)

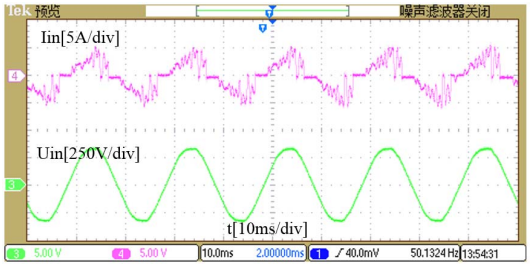

Fig.20 Input voltage and input current. (2000rpm, 2N.m)

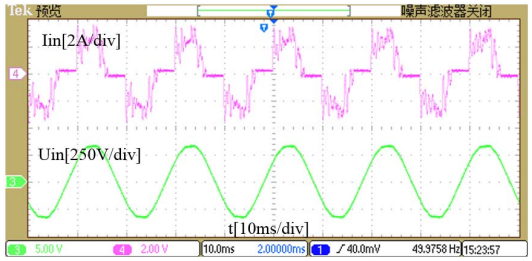

Fig.21 Input voltage and input current. (3000rpm, 0.5N.m)

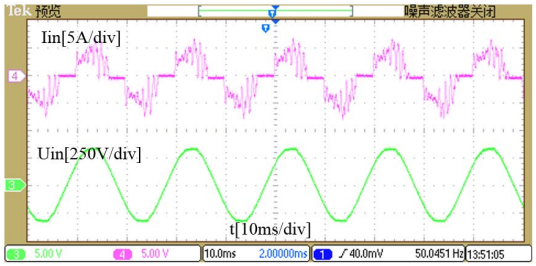

Fig.22 Input voltage and input current. (3000rpm, 2N.m)

Table 3.

PF	0.5N.m	2N.m
2000rpm	0.87	0.906
3000rpm	0.9	0.912

VI. CONCLUSIONS

This paper proposes a novel control strategy for the brushless DC motor drive system fed by electrolytic capacitor-less inverter. The use of E-cap-less extends the system lifetime, and does good to the power factor improvement. By regulating the inverter input current and applying the PWM_ON_PWM pattern, the high power factor of this system is achieved. The proposed method has a high power factor at various speed and load torque. The simulation and experimental results are given to demonstrate the validity of the proposed strategy for this BLDCM drive system without electrolytic capacitor.

REFERENCES

[1] Haga H, Yokoyama T, Shibata J, et al. High power factor control for single-phase to three-phase power converter without reactor and electrolytic capacitor [J]. 2008:766-771.

[2] Inazuma K, Ohishi K, Haga H. High-power-factor control for inverter output power of IPM motor driven by inverter system without electrolytic capacitor[C].IEEE International Symposium on Industrial Electronics. IEEE, 2011:619-624.

[3] Hiraide T, Ohishi K, Haga H. Input harmonic current reduction method for electrolytic capacitor-less inverter for IPMSM drive system[C]. IEEE International Symposium on Industrial Electronics. IEEE, 2013:1-6.

[4] Abe K, Ohishi K, Haga H. Fine current harmonics suppression control for the input current of electrolytic capacitor-less inverter for IPMSM[C]. Industrial Electronics Society, IECON 2015 -, Conference of the IEEE. IEEE, 2015:000777-000782.

[5] Abe K, Ohishi K, Haga H. Input current harmonics reduction control for electrolytic capacitor less inverter based IPMSM drive system[C]. International Power Electronics Conference. 2014:3153-3158.

[6] Wang S, Lee A C. A 12-Step Sensorless Drive for Brushless DC Motors Based on Back-EMF Differences[J]. IEEE Transactions on Energy Conversion, 2014, 1(2):646-654.

[7] Lee W J, Sul S K. A New Starting Method of BLDC Motors Without Position Sensor[J]. IEEE Transactions on Industry Applications, 2006, 42(6):1532-1538.

[8] Promthong S, Konghirun M. A PWM technique to minimize torque ripple in BLDC motor for low-cost applications[C]. International Conference on Electrical Engineering/electronics, Computer, Telecommunications and Information Technology. IEEE, 2013:1-6.

[9] Sheng T, Wang X, Shan T. A new method to reduce both conduction and commutation torque ripple for BLDC machines[C]. International Conference on Electrical Machines and Systems. IEEE, 2015:2975-2980.

[10] Li G, Liu J, Wang S. Investigation on Leading Angle Flux Weakening Control of Brushless DC Motor[C]. International Conference on Measuring Technology and Mechatronics Automation. IEEE, 2010:524-527.

[11] Kong H, Cui G, Zheng A. Field-Weakening Speed Extension of BLDCM Based on Instantaneous Power Theory[C]. International Conference on Electrical and Control Engineering. IEEE, 2010:3753-3756.

[12] Wei Y, Xu Y, Zou J, et al. Current limit strategy for BLDC motor drive with minimized dc-link capacitor[C]. International Conference on Electrical Machines and Systems. IEEE, 2014:1082-1086.